STEM CELLS®
Original Article

Electrophysiological Properties of Pluripotent Human and Mouse Embryonic Stem Cells

KAI WANG,[a] TIAN XUE,[b] SUK-YING TSANG,[b] RIKA VAN HUIZEN,[b] CHUN WAI WONG,[a] KEVIN W. LAI,[a] ZHAOHUI YE,[d] LINZHAO CHENG,[d] KA WING AU,[a] JANET ZHANG,[a] GUI-RONG LI,[a] CHU-PAK LAU,[a] HUNG-FAT TSE,[a] RONALD A. LI[b,c]

[a]Department of Medicine, University of Hong Kong, Hong Kong, China; Departments of [b]Medicine and [c]Cellular and Molecular Medicine and [d]Institute for Cell Engineering, Johns Hopkins University, Baltimore, Maryland, USA

Key Words. Embryonic stem cells • Electrophysiology • Pluripotency • Ion channels

ABSTRACT

Pluripotent embryonic stem cells (ESCs) possess promising potential for cell-based therapies, but their electrophysiological properties have not been characterized. Here we describe the presence of ionic currents in mouse (m) and human (h) ESCs and their physiological function. In mESCs, tetraethylammonium (TEA)–sensitive depolarization-activated delayed rectifier K^+ currents (IK_{DR}) (8.6 ± 0.9 pA/pF at +40 mV; IC_{50} = 1.2 ± 0.3 mM), which contained components sensitive to 4-aminopyridine (4-AP) (IC_{50} = 0.5 ± 0.1 mM) and 100 nM Ca^{2+}-activated K^+ current (IK_{Ca}) blocker iberiotoxin (IBTX), were detected in 52.3% of undifferentiated cells. IK_{DR} was similarly present in hESCs (~100%) but with an approximately sixfold higher current density (47.5 ± 7.9 pA/pF at +40 mV). When assayed by bromodeoxyurindine incorporation, application of TEA, 4-AP, or IBTX significantly reduced the proliferation of mESCs and hESCs in a dose-dependent manner ($p < .05$). A hyperpolarization-activated inward current (I_h) (–2.2 ± 0.4 pA/pF at –120 mV) was detected in 23% of mESCs but not hESCs. Neither Na_v nor Ca_v currents were detected in mESCs and hESCs. Microarray and reverse transcription–polymerase chain reaction analyses identified several candidate genes for the ionic currents discovered. Collectively, our results indicate that pluripotent ESCs functionally express several specialized ion channels and further highlight similarities and differences between the two species. Practical considerations for the therapeutic use of ESCs are discussed.
STEM CELLS *2005;23:1526–1534*

INTRODUCTION

Embryonic stem cells (ESCs) are derived from the inner cell mass of blastocysts. Because ESCs can propagate indefinitely in culture while maintaining their pluripotency to differentiate into all cell types, they may therefore provide an unlimited supply of specialized cells such as cardiomyocytes and neurons for cell-based therapies. For instance, direct injection of pluripotent ESCs after myocardial infarction has been suggested as a means to repair the damaged heart [1]. However, transplantation of cells with undesirable electrical properties into the heart can predispose patients to lethal electrical disorders (arrhythmias) [2, 3]. Therefore, it is critical to understand the electrophysiological profile of undifferentiated ESCs, which has not been characterized. In this study, we hypothesize that ion channels are functionally expressed in mouse (m) and human (h) ESCs, although the specific encoding genes (and/or their isoforms) and their expression levels might differ. We discovered that several specialized ion channels are differentially expressed in pluripotent mESCs and hESCs. Collectively, our experiments reveal further similarities and differences between the two species. We discuss these results in rela-

Correspondence: Ronald Li, Ph.D., Johns Hopkins University, 720 Rutland Avenue, Ross 1165, Baltimore, Maryland 21205, USA. Telephone: 410-614-0035; Fax: 410-502-2802; e-mail: ronaldli@jhmi.edu; and Hung-Fat Tse, M.D., University of Hong Kong, Cardiology Division, Queen Mary Hospital, Pokfulam, Hong Kong. e-mail: hftse@hkucc.hku.hk Received October 27, 2004; accepted for publication June 12, 2005; first published online in STEM CELLS *EXPRESS* August 9, 2005. 1066-5099/2005/$12.00/0 doi: 10.1634/stemcells.2004-0299

tion to the physiological function of ion channels in hESC biology as well as practical considerations for potential therapeutic applications of hESCs.

Materials and Methods

Maintenance of mESCs and hESCs

The mESC line R1 [4] (kind gift from Dr. Andras Nagy, University of Toronto, Toronto), which has been genetically engineered to constitutively express the green fluorescent protein (GFP), was used in this study to assist their identification from mouse embryonic fibroblast (MEF) cells. mESCs were maintained in their undifferentiated stage by growing on mitomycin-treated MEF feeder layer [5] in Dulbecco's modified Eagle's medium (DMEM) (GIBCO, Carlsbad, CA, http://www.lifetech.com) supplemented with 20% fetal bovine serum (GIBCO), 2 mM L-glutamine, 1 mM sodium pyruvate, 0.1 mM β-mercaptoethanol, 0.1 mM nonessential amino acids, and 1,000 U/ml leukemia inhibitory factor (Chemicon, Temecula, CA; http://www.chemicon.com).

For hESCs, the H1 line (WiCell Research Institute, Madison, WI, http://www.wicell.org) [6] that has been stably transduced by the recombinant lentivirus LV-CAG-GFP (see below for further description of the lentiviral vector used), as we have recently described, was used [7, 8]. hESCs were maintained on irradiated MEF feeder layer and propagated as previously described. The culture medium consisted of DMEM supplemented with 20% fetal bovine serum (HyClone, Logan, UT, http://www.hyclone.com), 2 mM L-glutamine, 0.1 mM β-mercaptoethanol, and 1% nonessential amino acids. MEF cells were obtained from 13.5-day-old embryos of CF-1 mice.

Lentivirus-Mediated Stable Genetic Modification of hESCs

For stable genetic modification, we used the self-inactivating HIV1-based lentiviral vector (LV) [9]. The plasmid pLV-CAG-GFP was created from pRRL-hPGK-GFP SIN-18 (generously provided by Dr. Didier Trono, University of Geneva, Geneva, Switzerland) by replacing the human phosphoglycerate kinase 1 (hPGK) promoter with the CAG promoter, an internal composite constitutive promoter containing the cytomegalovirus enhancer and the β-actin promoter. Recombinant lentiviruses were generated using the three-plasmid system [10] by cotransfecting HEK293T cells with pLenti-CAG-GFP, pMD.G, and pCMVΔR8.91. The latter plasmids encode the vesicular stomatitis virus G envelope protein and the HIV-1 *gag/pol, tat,* and *rev* genes required for efficient virus production, respectively. Lentiviral particles were harvested by collecting the culture medium at 48 hours after transfection and were stored at –80°C before use.

hESCs were transduced by adding purified lentiviruses to cells at a final concentration of 10,000 TU ml^{-1} with 8 μg/ml polybrene to facilitate transduction. The multiplicity of infection was approximately 5 for each round of transduction. After 4–6 hours of incubation with LV-CAG-GFP, 2 ml fresh medium per 60 mm dish was added. Transduction was allowed to proceed for at least 12–16 hours. Cells were washed with phosphate-buffered saline (PBS) twice to remove residual viral particles. For generating stably LV-CAG-GFP–transduced hESCs, green portions of hESC colonies were microsurgically segregated from the nongreen cells, followed by culturing under undifferentiating conditions for expansion. This process was repeated until a homogenous population of green hESCs, as confirmed by fluorescence-activated cell sorter, was obtained. Further details are also provided in another recent publication [11].

Immunostaining

mESCs or hESCs were fixed in 4% paraformaldehyde for 15 minutes at 21°C, washed with PBS, and permeabilized with 0.1% Trition X-100/PBS. The cells were then blocked with 10% bovine serum albumin with 0.075% saponin or 4% goat serum in PBS for 2 hours at 21°C. Fixed cells were incubated with the primary antibodies at a dilution of 1:25 (for SSEA-4 and TRA-1-60 in hESC staining) (Chemicon) overnight at 4°C, followed by incubation with fluorescent-labeled secondary antibodies for 50 minutes at 21°C and visualization by laser-scanning confocal microscopy.

Cell Proliferation Assay

Cell proliferation was determined in 96-well plates using a nonradioactive chemiluminescent bromodeoxyurindine (BrdU) kit (Roche Diagnostics, Basel, Switzerland, http://www.roche-applied-science.com) according to the manufacturer's protocols. mESCs or hESCs were treated with specified concentrations of tetraethylammonium (TEA), 4-aminopyridine (4-AP), or iberiotoxin (IBTX) for 24 hours. BrdU labeling solution was then added to give a final concentration of 10 μM of BrdU. Medium was removed after 2 hours, and cells were fixed with the addition of FixDenat solution (Roche Dianostics) for 30 minutes at room temperature. After removing FixDenat, 100 μl freshly diluted 1:100 anti-BrdU peroxidase solution was added to the wells for 30 minutes, followed by washing three times. Finally, 100 μl of substrate solution was added, and luminescence was read by a multiwell scanning spectrophotometer automatic luminometer.

Cell viability was determined in 96-well plates using a colorimetric MTT [3-(4, 5-dimethylthiazolyl-2)-2, 5-diphenyltetrazolium bromide] kit (Roche Diagnostics). Briefly, specified concentrations of TEA, 4-AP, or IBTX were added for 24 hours. Then 10 μl of MTT labeling reagent (5 mg/ml in PBS) was added to each well, followed by incubation at 37°C for 4 hours. Solubilization solution (100 μl) was added to dissolve the formazan crystals formed. Absorbances at 540 nm were read by a spectrophotometer. Untreated cells were used as control (i.e., 100% survival).

Electrophysiology

Only GFP-expressing mESCs and hESCs (~15 pF) were selected for experiments. Electrophysiological recordings were performed at room temperature using whole-cell patch clamp. Pipette electrodes (TW120F-6; World Precision Instruments, Sarasota, FL, http://www.wpiinc.com) were fabricated using a Sutter P-87 horizontal puller and fire-polished and had final tip resistances of 2–4 MΩ. All recordings were performed at room temperature in a bath solution containing (in mM) NaCl 110, KCl 30, $CaCl_2$ 1.8, $MgCl_2$ 0.5, HEPES 5, and glucose 10, pH adjusted to 7.4 with NaOH. The internal solution for patch recordings contained (in mM) NaCl 10, KCl 130, $MgCl_2$ 0.5, HEPES 5, EGTA 1, and MgATP 5, pH adjusted to 7.3 with KOH. For recording Ca^{2+}-activated large-conductance K^+ current (IK_{Ca}), 2.5 mM Ca^{2+} was added to the pipette solution containing (in mM) K-aspartate 110, NaCl 10, KCl 20, $MgCl_2 \cdot 6H_2O$ 1, Na_2-phosphocreatine 5, HEPES 10, K_2-EGTA 5, Mg_2ATP 5, and GTP 0.1, pH adjusted to 7.2 with KOH. Blockers were diluted to the final concentrations in the bath solution as indicated and administrated via superfusion (at least 10 ml) using a fast-exchange perfusion system. The current amplitude at +50 mV was monitored every 30 seconds after 5 minutes of incubation until steady-state current blockage was achieved.

Half-blocking concentrations (IC_{50}) were determined from the following binding isotherm: $I = I_{blocker\text{-}ins} + (1 - I_{blocker\text{-}ins})/(1 + [blocker]/IC_{50})^n)$, in which IC_{50} is the half-blocking concentration, $I_{blocker\text{-}ins}$ is blocker-insensitive component, n is the Hill coefficient, and I_0 and I are the peak currents measured at the voltage indicated before and after application of the blocker, respectively. All IC_{50} and half-effective concentration (EC_{50}) values reported were calculated from individual determinations (i.e., curve fitting to data from individual experiments). The curves presented in the Figures were fitted to averaged data points pooled from all experiments.

Reverse Transcription–Polymerase Chain Reaction

Total RNA was prepared from mESCs or mouse brain using ToTALLY RNA Kit (Ambion Inc., Austin, TX, http://www.ambion.com). Single-stranded cDNA was synthesized from approximately 1 μg of total RNA using random hexamers and SuperScript reverse transcription (RT) (Invitrogen, Carlsbad, CA, http://www.invitrogen.com) according to the manufacturer's protocols, followed by polymerase chain reaction (PCR) amplification with gene-specific primers for ion channel genes. Primers, annealing temperatures, product sizes, and the corresponding references are given in Table 1. 18S ribosomal RNA (498 bp) was used as an internal control. The reaction was conducted using the following protocol: initial denaturing of the template for 5 minutes at 94°C followed by 32 repeating cycles of denaturing for 1 minute at 94°C, annealing for 1 minute, extension for 1 minute at 72°C, and a final elongation at 72°C for 7 minutes. The PCR products were size-fractionated by 1% agarose gel electrophoresis and visualized by ethidium bromide staining. All the primers were tested with preparations from mouse brain and water as positive and negative controls, respectively. To analyze RNA expression in hESCs by RT-PCR, total RNA was extracted using a NucleoSpin RNAII kit (Clontech, Palo Alto, CA, http://www.clontech.com), treated with DNase I, and used for RT-PCR with SuperScript One-Step RT-PCR with the Platinum *Taq* system (Invitrogen). The primers for gene-specific RT-PCR are given in Table 2. Equal aliquots of the PCR products were electrophoresed through 2% agarose gels and visualized by ethidium bromide staining.

Microarray Analysis

Microarray analysis was performed using Affymetrix human genome U133A array (Affymetrix, Santa Clara, CA http://www.affymetrix.com), which represents 18,400 transcript and variants, including 14,500 well-characterized human genes. Total RNA was extracted from pluripotent hESCs (H1) and hybridized to microarrays according to the protocols provided by the manufacturer. The software Genespring 6.0 (Silicon Genetics, Redwood City, CA, http://www.silicongenetics.com) was used for microarray data analysis. Data were normalized to the expression level of the 50th percentile of the entire chip and filtered to show genes that are labeled as expressed (i.e., present flags) as defined by Affymetrix analysis.

Statistics

All data reported are means ± SEM. Statistical significance was determined for all individual data points and fitting parameters using one-way analysis of variance and Tukey's Honestly Significantly Different post-hoc test at the 5% level.

Results

Ionic Currents in Pluripotent mESCs

Figure 1A shows that undifferentiated mESC colonies were homogenously immunostained for the pluripotency markers Oct-4 and SSEA-1 [12, 13]. In 159 of 304 (52.3%) undifferentiated mESCs, depolarization-activated time-dependent noninactivating outward currents that increased progressively with positive voltages could be recorded (8.6 ± 0.9 pA/pF at +40 mV; Figs. 1B, 1C). These outwardly rectifying currents resemble the delayed-rectifier K^+ currents (IK_{DR}) and could be dose-dependently inhibited by the known K^+ channel blocker TEA^+ [14, 15] (IC_{50} = 1.2 ± 0.3 mM, n = 13; Figs. 1B, 1D). IK_{DR} in mESCs was also sensitive to 4-AP (IC_{50} = 0.5 ± 0.1 mM, n = 17), a more potent K channel blocker than TEA^+ [16, 17], and the Ca^{2+}-activated large-conductance K^+ current (IK_{Ca}) blocker IBTX (100nM) (current inhibition = 33.2% ± 12.7%, n = 3) (Figs. 1B, 1E). As shown in Figures 1D and 1E, increasing TEA or 4-AP to 30 mM could not lead to complete current inhibition. Indeed, even combined application

Table 1. Mouse gene-specific primers for reverse transcription–polymerase chain reaction

Gene	Accession no.	Forward primer sequence (5'-3')	Reverse primer sequence (5'-3')	Length (bp)	Annealing temperature (°C)	Reference
HCN1	NM_010408	CTCTTTTTGCTAACGCCGAT	CATTGAAATTGTCCACCGAA	291	57	[46]
HCN2	NM_008226	GTGGAGCGAGCTCTACTCGT	GTTCACAATCTCCTCACGCA	229	57	[46]
HCN3	NM_008227	GACACCCGCCTCACTGATGGAT	GTTTCCGCTGCAGTATCGAATTC	370	57	[46]
HCN4	XM_287905	TGCTGTGCATTGGGTATGGA	TTTCGGCAGTTAAAGTTGATG	337	47	[46]
Kv1.1	NM_010595	GCCTCTGACAGTGACCTCAGC	GGGACAGGAGTCGCCAAGGG	240	57	[47]
Kv1.2	NM_008417	CGTCCTCCCCTGACCTAAA	CCATGCAGAACCAGATGCTGTAG	296	57	[47]
Kv1.3	NM_008418	ATCTTCAAGCTCTCCCGCCA	CGATCACCATATACTCCGAC	478	53	[48]
Kv1.4	NM_021275	CTCCTCCCATGATCCTCAAGG	GCAGGTCTGTGTACGAACACC	257	57	[47]
Kv1.5	NM_145983	GCCATTGCCATCGTGTCGGT	ACATGTGGTCTCCACGATGA	242	53	[48]
Kv1.6	NM_013568	GCTTGGCAAACCTGACTTTGC	CCTGTTTTCCTGCAGGCC	136	57	[47]
Kv2.1	NM_008420	CGGCAGTTCAACCTGATCCC	TTTATTGCCCAGAATGCTGTCG	468	57	[49]
Kv3.1	NM_008421	CGAGCTGGAGATGACCAAG	AAGAAGAGGGAGGCAAAGG	156	60	Designed with Primer Premier 5.0[a]
Kv3.2	U52223	AATAGCCATGCCTGTGC	AGCGTCTGATAGGGAGC	296	60	Designed with Primer Premier 5.0[a]
Kv4.2	NM_019697	ATCGCCCATCAAGTCACAGTC	CCGACACATTGGCATTAGGAA	111	53	[50]
Kv4.3	NM_019931	CAAGACCACCTCACTCATCGA	TCGAGCTCTCCATGCAGTTCT	176	60	[50]
BK	NM_010610	CCATTAAGTCGGGCTGATTTAAG	CCTTGGGAATTAGCCTGCAAGA	188	53	[51]

[a] Manufactured by PREMIER Biosoft International, Palo Alto, CA, http://www.premierbiosoft.com.

Table 2. Human gene-specific primers for reverse transcription–polymerase chain reaction

Gene	Accession no.	Forward primer sequence (5'-3')	Reverse primer sequence (5'-3')	Length (bp)	Annealing temperature (°C)	Reference
Ca_v α2/δ *subunit 2*	NM_006030	gctgcagaactccaacatca	CGATGGAAGGGATCTCAAAA	224	60	Designed with Primer3a
Ca_v β3 *subunit*	U07139	acagcttgatgccctctgat	tggttgtgctctgagtcctg	211	60	Designed with Primer3a
$Ca_v2.1$	NM_023035	agtgaacaaaaacgccaacc	aaagtagcgcaggttcagga	184	60	Designed with Primer3a
$Na_v1.9$	NM_014139	ccaccaccaagagaaaggaa	tcagtcacagtggaccttgc	200	60	Designed with Primer3a
$K_v9.3$	NM_002252	CAGTGAGGATGCACCAGAGA	TTGCTGTGCAATTCTCCAAG	200	60	[52]
$K_v4.2$	NM_0012281	GCCAATGTGTCAGGAAGTCA	TTCTGGGGTGGTTACTGGAG	201	60	[52]
$K_v11.1$	NM_000238	CCTTCCTCTGCATTGCTTTT	CTTGTCTTGGGGTGAGCTGT	210	60	[52]
$K_v2.1$	NM_004975	ACAGAGCAAACCAAAGGAAGAAC	CACCCTCCATGAAGTTGACTTTA	383	60	[52]
$K_v7.2$	NM_172109	gcaagctgcagaatttcctc	agtactccacgccaaacacc	201	60	Designed with Primer3a
GAPDH	NM_013568	ACATCAAGAAGGTGGTGAAGCAGG	CTCTTGCTCTCAGATCCTTGCTGG	281	60	Designed with Primer3a
HCN1	NM_021072.1	GGCGGCAGTATCAAGAGAAG	GGCATTGTAGCCACCAGTTT	211	60	Designed with Primer3a

[a] For information about Primer3 visit http://fokker.wi.mit.edu/cgi-bin/primer3/primer3_www.cgi.

of 30 mM TEA and 30 mM 4-AP also could not completely eliminate the IK_{DR} (30 mM 4-AP, 30 mM TEA, and 30 mM TEA + 30 mM 4-AP reduced the IK_{DR} to 45.8% ± 2.1%, 39.3% ± 7.6%, and 45.1% ± 8.1%, respectively; $p > .05$). The currents remaining after combined TEA/4-AP blockade were also not sensitive to 1 mM $BaCl_2$, implicating the presence of some background current.

Although voltage-gated Na^+ (Na_v) and Ca^{2+} (Ca_v) currents were completely absent in all pluripotent mESCs tested ($n > 200$), whether IK_{DR} was present (Fig. 1B) or not (Fig. 2A), a modest yet detectable hyperpolarization-activated inward current (I_h, encoded by the hyperpolarization-activated cyclic nucleotide-modulated nonselective or HCN ion channel family [18]; –2.2 ± 0.4 pA/pF at –120 mV) was detected in 79 of 270 cells (29.3%; Fig. 2B). I_h in mESCs was reversibly blocked by the HCN inhibitor Cs^+ [19, 20]. Application of 1 μM isoproterenol altered neither the kinetics nor amplitude of I_h recorded in mESCs. Inwardly rectifying K currents (I_{K1}) responsible for stabilizing the resting membrane potential were also not present.

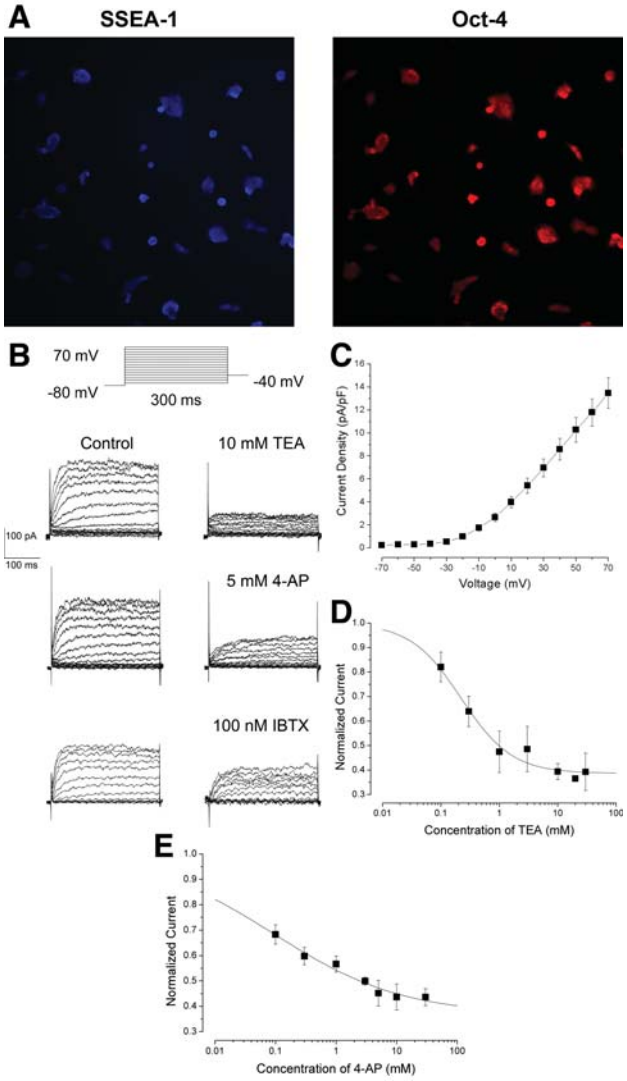

Figure 1. (A): Images of pluripotent mESCs immunostained for SSEA-1 and Oct-4. **(B):** Representative current tracings recorded from undifferentiated mESCs before (left panels) and after (right panels) blockade by TEA, 4-AP, and IBTX, as indicated. The electrophysiological protocol used for eliciting currents is also given. **(C):** Current-voltage relationship of IK_{DR} of mESCs. Dose–response relationships for **(D)** TEA and **(E)** 4-AP block of IK_{DR} of mESCs. Abbreviations: 4-AP, 4-aminopyridine; IBTX, iberiotoxin; mESC, mouse embryonic stem cell; TEA, tetraethylammonium.

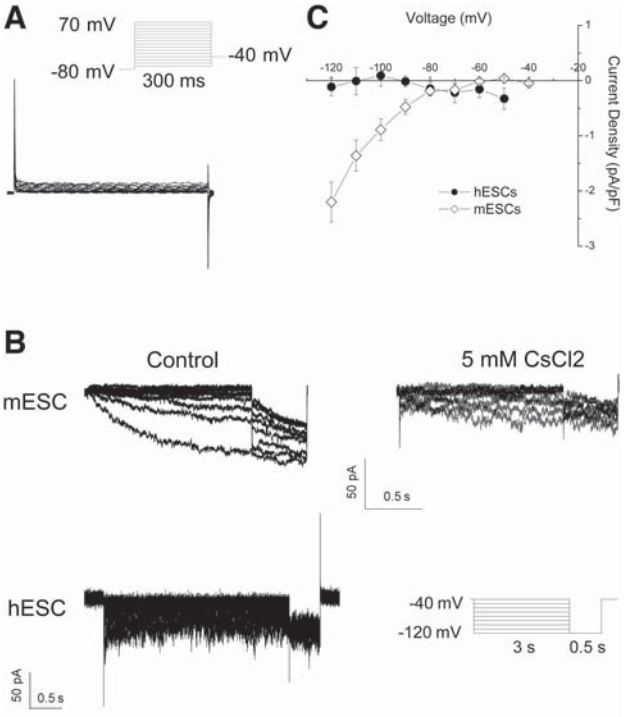

Figure 2. (A): Stimulation protocol and representative current traces demonstrating the absence of Na_v or Ca_v currents in an mESC that lacks IK_{DR}. **(B):** $CsCl_2$-sensitive hyperpolarization-activated currents could be recorded from pluripotent mESCs but not hESCs. **(C):** Steady-state current-voltage relationships of hyperpolarization-activated currents of mESCs and hESCs. Abbreviations: hESC, human embryonic stem cell; mESC, mouse embryonic stem cell.

To obtain insights into the molecular identities of the ionic currents identified, total RNA was isolated from pluripotent mESCs for RT-PCR. Figure 3A shows that Kv1.1, 1.2, 1.3, 1.4, 1.6, 4.2, and BK (or Maxi-K) transcripts but not Kv1.5, 2.1, 3.1, 3.2, and 4.3 were detected. Consistent with the presence of I_h, HCN2 and HCN3 transcripts were also expressed. Inhibition by 4-AP and insensitivity to extracellular TEA ions is a pharmacological hallmark of A-type currents [21]. However, neither TEA-subtracted nor 4-AP–subtracted current traces from IK_{DR} blockade revealed any transient outward current with the typical rapid inactivation feature (data not shown). Therefore, although Kv1.1, 1.2, 1.6, and BK channels might underline the delayed rectifier current recorded, we conclude that Kv1.4- and Kv4.2-encoded transient outward K^+ currents were not functionally expressed.

Effects of Ion Channel Blockers

To investigate possible physiological roles of the ionic currents identified, we next studied the functional consequences of their pharmacological blockade by assessing the effects of extracellular application of K^+ channel blockers on cell proliferation. Specifically, we measured DNA synthesis as an index for replication by quantifying BrdU incorporation into genomic DNA during the S phase of the cell cycle, which is proportional to the rate of cell division [22]. Application of TEA^+ significantly inhibited the proliferation of mESCs in a dose-dependent manner (Fig. 3B, open squares). The EC_{50} was 20.1 ± 3.7 mM ($n = 3$), approximately 20-fold higher than the IC_{50} for IK_{DR} inhibition. Similarly, 4-AP (EC_{50} = 2.7 ± 0.2 mM; Fig. 3C, open squares) and IBTX (EC_{50} = 133.9 ± 25.9 nM; Fig. 3D, open squares) also dose-dependently reduced cell proliferation. Of note, the rank orders of these agents to inhibit proliferation follow the trend of their potencies to block IK_{DR} (i.e., IBTX > 4-AP > TEA). To assess the cytotoxic effect of K^+ channel

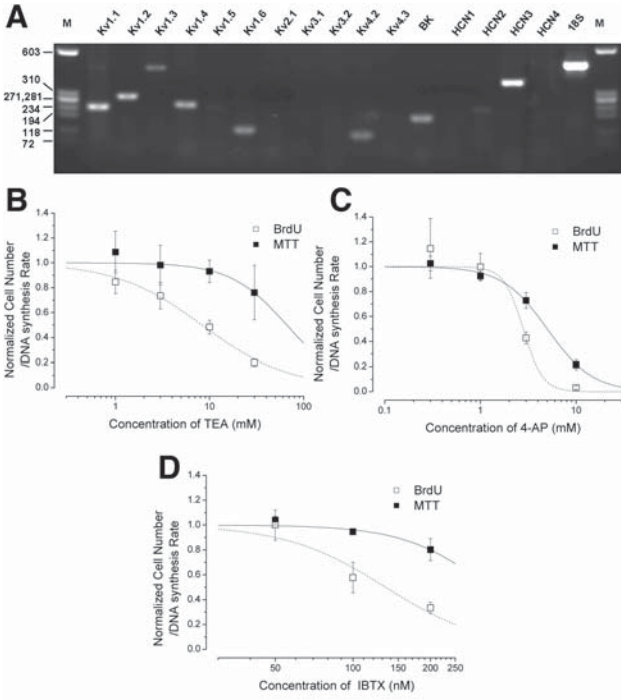

Figure 3. (A): Expression of ion channel transcripts in mESCs probed by semiquantitative reverse transcription–polymerase chain reaction. Dose–response relationships of **(B)** TEA, **(C)** 4-AP, and **(D)** IBTX for inhibition of mESC proliferation assessed by BrdU incorporation (open squares) and cytotoxic effects by MTT (solid squares). Abbreviations: 4-AP, 4-aminopyridine; BrdU, bromodeoxyurindine; IBTX, iberiotoxin; mESC, mouse embryonic stem cell; TEA, tetraethylammonium.

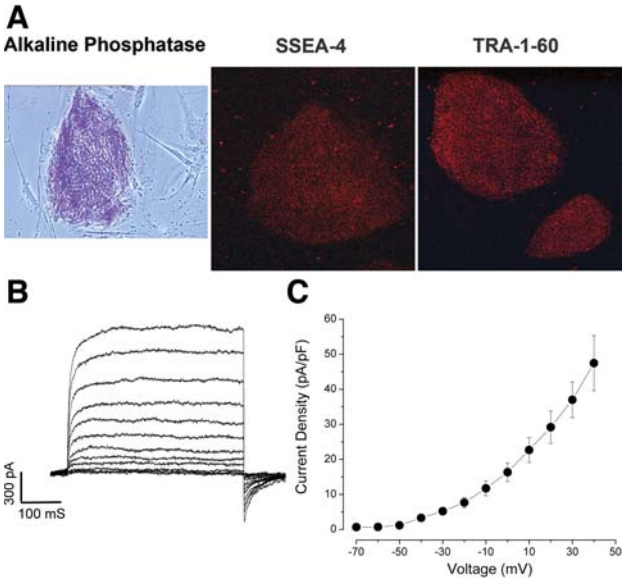

Figure 4. (A): Pluripotent hESCs were positive for alkaline phosphatase, SSEA-4, and TRA-1-60. **(B):** Representative current tracings recorded from undifferentiated hESCs. The same electrophysiological from Figure 1 was used. **(C):** Steady-state current-voltage relationship of IK_{DR} in hESCs. **(D):** IC_{50} for blockade of IK_{DR} and EC_{50} for proliferation inhibition by tetraethylammonium in hESCs. Abbreviation: hESC, human embryonic stem cell.

blockers, a colorimetric MTT kit was used to examine for changes in metabolism. Notably, the EC_{50} values for inhibition of metabolic activity by TEA (62.7 ± 9.0 mM; Fig. 3B, solid squares), 4-AP (4.6 ± 0.5 mM; Fig. 3C, solid squares), and IBTX (333.9 ± 64.6 nM; Fig. 3D, solid squares) were significantly higher than those for inhibiting cell proliferation ($p < .05$). These results implicate that the metabolic influences of these blockers were relatively insignificant at concentrations at which they effectively exert their inhibitory effects on ESC proliferation, presumably by K^+ channel blockade.

Electrophysiological Properties of hESCs: Similarities and Differences

Although hESCs and mESCs share several similarities, significant differences are known to exist between the two species [23]. Therefore, we also examined the previously unexplored electrophysiological properties of hESCs. Pluripotent hESCs were positive for markers such as alkaline phosphatase, Oct4, SSEA4, and TRA-60 (Fig. 4A), consistent with previous reports [6]. Similar to mESCs, TEA^+-sensitive IK_{DR} (IC_{50} = 2.1 ± 0.2 mM; Fig. 4D) was also detected in hESCs (~100%), but the current density was approximately sixfold higher (47.5 ± 7.9 pA/pF at +40 mV, $n = 12$, $p < .05$) (Figs. 4B, 4C). Similar to mESCs, application of TEA^+ dose-dependently inhibited hESC proliferation as assayed by BrdU incorporation, with an EC_{50} (11.6 ± 2.0 mM) (Fig. 4D). Unlike mESCs, however, there was no measurable I_h in all hESCs tested ($n = 30$; Fig. 2B). Same as mESCs, neither Na_v nor Ca_v currents could be detected in hESCs.

Microarray Analysis of Ion Channel Genes in hESCs

Using Affymetrix U133A chips, we performed microarray analysis of pluripotent hESCs to examine the expression of ion channels at the transcriptomic level. Figure 5A shows the expression profile of all genes tested in undifferentiated hESCs. For voltage-gated ion channels, a total of 36, 19, and 49 genes on the U133A chips were identified as Ca_v, Na_v, or K_v channel genes, respectively. For inspection, their expression profile is extracted in Figure 5A and further summarized in Figures 5B and 5C by normalizing signals to the average expression level of the entire microarray in a manner similar to that of cytokines and their receptors in hESCs, as recently reported by Dvash et al. [24]. Our data indicate that among the total 104 voltage-gated ion channel genes mentioned above, only the transcripts of 3, 1, and 5 Ca_v, Na_v, and K_v genes were significantly expressed, as defined by Affymetrix. The corresponding gene products were CACNA1A ($Ca_v2.1$), CACNA2D2 (Ca_v α2/δ subunit 2), CACNB3 (Ca_v β3 subunit), SCN11A ($Na_v1.9$), KCNB1 ($K_v2.1$), KCND2 ($K_v4.2$), KCNQ2 ($K_v7.2$), KCNS3 ($K_v9.3$), and KCNH2 ($K_v11.1$) (note, however, that I_{Ca}, I_{Na}, and Kv4.2-encoded transient outward K^+ currents could not be electrophysiologically

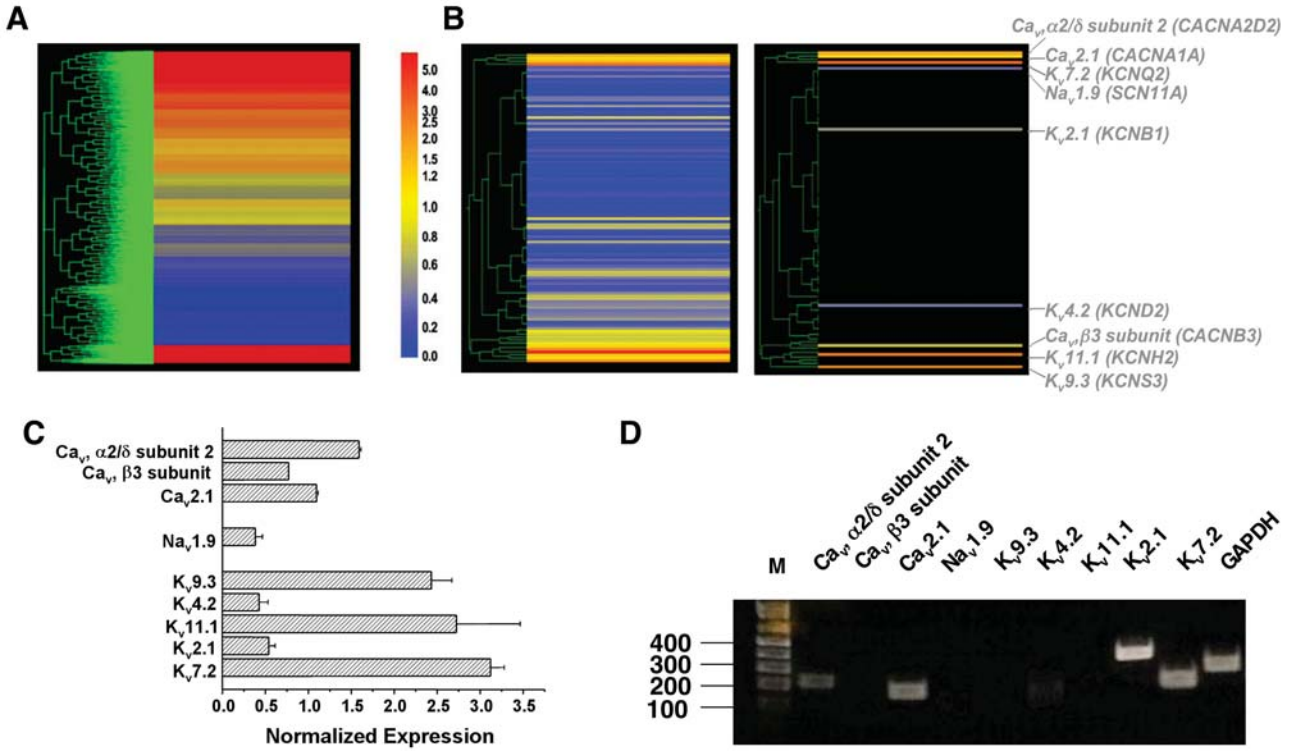

Figure 5. (A): Microarray analysis of pluripotent hESCs for the transcript expression of all genes tested using Affymetrix U133A microarrays (see Materials and Methods). **(B):** Left, 104 voltage-gated Ca_v, Na_v, and K_v channel genes are clustered. The same expression scale bar shown in **(A)** was used. Right, same as the left panel, except only transcripts that were defined to be expressed, as defined by Affymetrix, are shown. **(C):** Bar graph of normalized transcript levels of the expressed ion channel genes. Data were normalized to the expression level of the 50th percentile of the entire microarray. **(D):** Expression of ion channel transcripts in hESCs probed by semiquantitative reverse transcription–polymerase chain reaction. Abbreviation: hESC, human embryonic stem cell.

recorded, like mESCs). Of note, KCNQ2 and KCNH2, which underlie the noninactivating, slowly deactivating M-current [25] and the rapid component of the cardiac delayed rectifier (IK_r) [26], were relatively highly expressed. Similarly, KCNB1 and KCNS3, which encode for the delayed rectifier $K_v2.1$ channels and the silent modulatory α-subunit $K_v9.3$ that heteromerizes with $K_v2.1$ subunits [27–29], respectively, were also expressed. Collectively, these ion channel genes could underlie the K_{DR} current identified, although further experiments will be needed to confirm and dissect their molecular identities. By contrast, no HCN transcript was expressed in pluripotent hESCs. RT-PCR confirmed the array results for five of nine channels (Fig. 5D).

Discussion

In this report, we have demonstrated that undifferentiated ESCs express several specialized ion channels at the mRNA and functional levels. Although cultured undifferentiated mESCs and hESCs were relatively homogenous when immunostained for pluripotency markers, heterogeneous expression of ion channels was observed in mESCs: Only fractions of mESCs tested express measurable IK_{DR} and I_h. This observation parallels the heterogeneous pattern of ion channel expression recently described for human mesenchymal stem cells (hMSCs) [30]. Unlike mESCs (and hMSCs), however, ion channel expression in hESCs seems to be much more homogenous. IK_{DR} was recorded in all pluripotent hESCs tested (vs. 52.3% of mESCs). In addition to the higher occurrence, the expressed amplitude of IK_{DR} was also approximately 10-fold higher in hESCs, which in turn could underlie the more potent effects of K^+ channel blockers on cell proliferation. Of note, high concentrations of TEA^+ and IBTX also led to cytotoxic effects. Both the cytotoxicity of K^+ channel antagonists and their effects on cell proliferation could result from their cellular uptake (e.g., via endocytosis) followed by interactions with some intracellular targets other than K channels. In this regard, K^+ channel blockers are anticipated not to affect mESCs that do not express IK_{DR} if the resultant functional consequences arise solely from their blockade of K^+ channels. Unfortunately, our experiments do not dissect the relative contribution of these possibilities because the two cell populations cannot be readily isolated. In addition, tail currents were more often seen in hESCs rather than mESCs. Different channels, as suggested by our microarray and RT-PCR data, are likely to underlie these human and mouse delayed rectifier currents. Further experiments (e.g., the use of small interfering RNA and/or dominant-negative ion channel constructs [31] to suppress the surface expression of ion

channel receptors) will be required to address the above-mentioned questions and to dissect their precise molecular identities.

Although self-renewable ESCs may provide an unlimited supply of cells for transplantation, this promising potential is somewhat hampered by concerns that ESCs (and their multipotent derivatives) also possess the potential to form malignant tumors. Various lines of evidence have suggested that K channels provide a link between physiological and biochemical processes that regulate cell cycle and proliferation by influencing the resting membrane potential (e.g., hyperpolarization is required for the progression of certain cells into the G1 phase of the mitotic cycle) in several vastly different cell types from cancer to T lymphocytes [32–36]. In accordance with this notion, our results show that pharmacologic blockade of IK_{DR} also inhibits the proliferation of both hESCs and mESCs. Perhaps targeted inhibition of specific K channel activity (e.g., by genetic suppression via overexpression of particular dominant-negative ion channel constructs [31]) may lead to a novel strategy to arrest any undesirable cell division of and to cause cytotoxicity in pluripotent ESCs, thereby inhibiting or eliminating their tumorgenicity.

Not surprisingly, the transcript expression profiles of mESCs and hESCs do not always correspond to the functional expression profile of ion channels. Previously, van Kempen et al. [37] demonstrated that a variety of ion channel transcripts, such as those of Kv4.3, KvLQT1, Na_v, and HCN channels, are present in pluripotent mESCs but no ionic currents at all can be detected electrophysiologically before differentiation is induced [37]. Similarly, a direct correlation between mRNA and membrane ionic currents is also not seen in the pluripotent P19 embryonic carcinoma cell line [38]. Nevertheless, time-dependent changes in ion channel mRNA expression upon in vitro differentiation of hESCs have been reported [39]. The differences between these observations and those presented here could be attributed to the different pluripotent cell lines investigated or the different culturing conditions used, which may likewise contribute to the species differences in the electrophysiological profiles observed between mESCs and hESCs.

Although injection of undifferentiated mESCs into mice does not seem to be arrhythmogenic (unpublished data) [1], the associated electrophysiological consequences could be masked due to the slow current kinetics of IK_{DR} in ESCs relative to the high mouse heart rate (~600 bpm) and thus extremely short cardiac cycles. Such arrhythmogenic potential could become prominent in species whose heart rates are much slower (e.g., ~80 bpm for humans). Like MSCs [40], pluripotent ESCs also express gap junction proteins [41–43] for electrical coupling. Furthermore, ESCs can even subsequently differentiate into electrically active lineages [7, 39, 44, 45]. Taken collectively, our present results highlight additional similarities and differences between mESCs and hESCs and further suggest that the electrophysiological profile, in addition to the tumorgenic potential, of a given undifferentiated hESC line needs to be carefully assessed before it can be used for therapeutic application, especially when organs or systems in which electrical coordination is key for their functions (e.g., cardiac, pancreatic, and neuronal) are involved.

Acknowledgments

K.W. and T.X. contributed equally to this study. This work was supported by grants from the National Institutes of Health (R01 HL-52768 and R01 HL-72857 to R.A.L.), the Blaustein Pain Research Centre (to R.A.L.), and the Hong Kong Research Grant Council (HKU 7459/04M to H.F.T., R.A.L., G.R.L., and C.P.L.). S.Y.T. was supported by a postdoctoral fellowship award from the Croucher Foundation. We would also like to thank Dr. Guibin Chen at Johns Hopkins for helpful discussion in microarray analysis.

Disclosures

The authors indicate no potential conflicts of interest.

References

1 Hodgson DM, Behfar A, Zingman LV et al. Stable benefit of embryonic stem cell therapy in myocardial infarction. Am J Physiol Heart Circ Physiol 2004;287:H471–H479.

2 Menasche P, Hagege AA, Vilquin JT et al. Autologous skeletal myoblast transplantation for severe postinfarction left ventricular dysfunction. J Am Coll Cardiol 2003;41:1078–1083.

3 Smits PC, van Geuns RJ, Poldermans D et al. Catheter-based intramyocardial injection of autologous skeletal myoblasts as a primary treatment of ischemic heart failure: clinical experience with six-month follow-up. J Am Coll Cardiol 2003;42:2063–2069.

4 Nagy A, Rossant J, Nagy R et al. Derivation of completely cell culture-derived mice from early-passage embryonic stem cells. Proc Natl Acad Sci U S A 1993;90:8424–8428.

5 Doetschman TC, Eistetter H, Katz M et al. The in vitro development of blastocyst-derived embryonic stem cell lines: formation of visceral yolk sac, blood islands and myocardium. J Embryol Exp Morphol 1985;87: 27–45.

6 Thomson JA, Itskovitz-Eldor J, Shapiro SS et al. Embryonic stem cell lines derived from human blastocysts. Science 1998;282:1145–1147.

7 Xue T, Cho HC, Akar FG et al. Functional integration of electrically active cardiac derivatives from genetically engineered human embryonic stem cells with quiescent recipient ventricular cardiomyocytes: insights into the development of cell-based pacemakers. Circulation 2005;111:11–20.

8 Moore JC, van Laake LW, Braam SR et al. Human embryonic stem cells: genetic manipulation on the way to cardiac cell therapies. Reprod Toxicol 2005;20:377–391.

9 Trono D. Lentiviral Vectors. New York: Spring-Verlag, 2002.

10 Zufferey R, Dull T, Mandel RJ et al. Self-inactivating lentivirus vector for safe and efficient in vivo gene delivery. J Virol 1998;72:9873–9880.

11 Moore JC, van Laake LW, Braahm SR et al. Human embryonic stem cells: genetic manipulation on the way to cardiac cell therapies. Reprod Toxicol 2005;20:377–391.

12 Solter D, Knowles BB. Monoclonal antibody defining a stage-specific mouse embryonic antigen (ssea-1). Proc Natl Acad Sci U S A 1978;75:5565–5569.

13 Niwa H, Miyazaki J, Smith AG. Quantitative expression of oct-3/4 defines differentiation, dedifferentiation or self-renewal of ES cells. Nat Genet 2000;24:372–376.

14 Hille B. The selective inhibition of delayed potassium currents in nerve by tetraethylammonium ion. J Gen Physiol 1967;50:1287–1302.

15 Kirsch GE, Taglialatela M, Brown AM. Internal and external tea block in single cloned K^+ channels. Am J Physiol 1991;261:C583–C590.

16 Mathie A, Wooltorton JRA, Watkins CS. Voltage-activated potassium channels in mammalian neurons and their block by novel pharmacological agents. Gen Pharmacol 1998;30:13–24.

17 Baker M, Howe JR, Ritchie JM. Two types of 4-aminopyridine-sensitive potassium current in rabbit schwann cells. J Physiol 1993;464:321–342.

18 Pape H-C. Queer current and pacemaker: the hyperpolarization-activated cation current in neurons. Annu Rev Physiol 1996;58:299–327.

19 Champigny G, Bois P, Lenfant J. Characterization of the ionic mechanism responsible for the hyperpolarization-activated current in frog sinus venosus. Pflugers Arch 1987;410:159–164.

20 McCormick DA, Pape HC. Properties of a hyperpolarization-activated cation current and its role in rhythmic oscillation in thalamic relay neurones. J Physiol 1990;431:291–318.

21 Amberg GC, Koh SD, Imaizumi Y et al. A-type potassium currents in smooth muscle. Am J Physiol Cell Physiol 2003;284:C583–C595.

22 Yu CC, Woods AL, Levison DA. The assessment of cellular proliferation by immunohistochemistry: a review of currently available methods and their applications. Histochem J 1992;24:121–131.

23 Boheler KR, Czyz J, Tweedie D et al. Differentiation of pluripotent embryonic stem cells into cardiomyocytes. Circ Res 2002;91:189–201.

24 Dvash T, Mayshar Y, Darr H et al. Temporal gene expression during differentiation of human embryonic stem cells and embryoid bodies. Hum Reprod 2004;19:2875–2883.

25 Cooper EC, Jan LY. M-channels: neurological diseases, neuromodulation, and drug development. Arch Neurol 2003;60:496–500.

26 Pond AL, Nerbonne JM. Erg proteins and functional cardiac I(kr) channels in rat, mouse, and human heart. Trends Cardiovasc Med 2001;11:286–294.

27 Kerschensteiner D, Monje F, Stocker M. Structural determinants of the regulation of the voltage-gated potassium channel kv2.1 by the modulatory alpha-subunit kv9.3. J Biol Chem 2003;278:18154–18161.

28 Kerschensteiner D, Stocker M. Heteromeric assembly of kv2.1 with kv9.3: effect on the state dependence of inactivation. Biophys J 1999;77:248–257.

29 Stocker M, Kerschensteiner D. Cloning and tissue distribution of two new potassium channel alpha-subunits from rat brain. Biochem Biophys Res Commun 1998;248:927–934.

30 Heubach JF, Graf EM, Leutheuser J et al. Electrophysiological properties of human mesenchymal stem cells. J Physiol 2004;554:659–672.

31 Xue T, Marban E, Li RA. Dominant-negative suppression of hcn1- and hcn2-encoded pacemaker currents by an engineered hcn1 construct: Insights into structure-function relationships and multimerization. Circ Res 2002;90:1267–1273.

32 Parihar AS, Coghlan MJ, Gopalakrishnan M et al. Effects of intermediate-conductance Ca^{2+}-activated k^+ channel modulators on human prostate cancer cell proliferation. Eur J Pharmacol 2003;471:157–164.

33 Vaur S, Bresson-Bepoldin L, Dufy B et al. Potassium channel inhibition reduces cell proliferation in the gh3 pituitary cell line. J Cell Physiol 1998;177:402–410.

34 Wonderlin WF, Strobl JS. Potassium channels, proliferation and g1 progression. J Membr Biol 1996;154:91–107.

35 Platoshyn O, Golovina VA, Bailey CL et al. Sustained membrane depolarization and pulmonary artery smooth muscle cell proliferation. Am J Physiol Cell Physiol 2000;279:C1540–C1549.

36 Vautier F, Belachew S, Chittajallu R et al. Shaker-type potassium channel subunits differentially control oligodendrocyte progenitor proliferation. Glia 2004;48:337–345.

37 van Kempen MJA, van Ginneken A, de Grijs I et al. Expression of the electrophysiological system during murine embryonic stem cell cardiac differentiation. Cell Physiol Biochem 2003;13:263–270.

38 van der Heyden MA, van Kempen MJ, Tsuji Y et al. P19 embryonal carcinoma cells: a suitable model system for cardiac electrophysiological differentiation at the molecular and functional level. Cardiovasc Res 2003;58:410–422.

39 Mummery C, Ward-van Oostwaard D, Doevendans P et al. Differentiation of human embryonic stem cells to cardiomyocytes: role of coculture with visceral endoderm-like cells. Circulation 2003;107:2733–2740.

40 Valiunas V, Doronin S, Valiuniene L et al. Human mesenchymal stem cells make cardiac connexins and form functional gap junctions. J Physiol 2004;555:617–626.

41 Sohl G, Theis M, Hallas G et al. A new alternatively spliced transcript of the mouse connexin32 gene is expressed in embryonic stem cells, oocytes, and liver. Exp Cell Res 2001;266:177–186.

42 Oyamada Y, Komatsu K, Kimura H et al. Differential regulation of gap junction protein (connexin) genes during cardiomyocytic differentiation of mouse embryonic stem cells in vitro. Exp Cell Res 1996;229:318–326.

43 Satin J, Kehat I, Caspi O et al. Mechanism of spontaneous excitability in human embryonic stem cell derived cardiomyocytes. J Physiol 2004;559:479–496.

44 Kehat I, Kenyagin-Karsenti D, Snir M et al. Human embryonic stem cells can differentiate into myocytes with structural and functional properties of cardiomyocytes. J Clin Invest 2001;108:407–414.

45 He JQ, Ma Y, Lee Y et al. Human embryonic stem cells develop into multiple types of cardiac myocytes: action potential characterization. Circ Res 2003;93:32–39.

46 Stieber J, Herrmann S, Feil S et al. The hyperpolarization-activated channel HCN4 is required for the generation of pacemaker action potentials in the embryonic heart. Proc Natl Acad Sci U S A 2003;100:15235–15240.

47 Smart SL, Bosma MM, Tempel BL. Identification of the delayed rectifier potassium channel, Kv1.6, in cultured astrocytes. Glia 1997;20:127–134.

48 Schilling T, Quandt FN, Cherny VV et al. Upregulation of Kv1.3 K(+) channels in microglia deactivated by TGF-beta. Am J Physiol Cell Physiol 2000;279:C1123–C1134.

49 Koh JT, Jeong BC, Kim JH et al. Changes underlying arrhythmia in the transgenic heart overexpressing Refsum disease gene-associated protein. Biochem Biophys Res Commun 2004;313:156–162.

50 Amberg GC, Koh SD, Hatton WJ et al. Contribution of Kv4 channels toward the A-type potassium current in murine colonic myocytes. J Physiol 2002;544:403–415.

51 Eghbali M, Toro L, Stefani E. Diminished surface clustering and increased perinuclear accumulation of large conductance Ca2+-activated K^+ channel in mouse myometrium with pregnancy. J Biol Chem 2003;278:45311–45317.

52 Platoshyn O, Remillard CV, Fantozzi I et al. Diversity of voltage-dependent k+ channels in human pulmonary artery smooth muscle cells. Am J Physiol Lung Cell Mol Physiol 2004;287:L226–L238.